SCIREA Journal of Electrical Engineering

http://www.scirea.org/journal/DEE

May 27, 2019

Volume 4, Issue 2, April 2019

Investigation of temperature and pressure dependence of thermodynamic parameters and Debye–Waller factor of CuAg72 alloy

Nguyen Ba Duc

Faculty of Physics, Tan Trao University, Vietnam

Email：ducnb@daihoctantrao.edu.vn

abstract

This study applies the anharmonic correlated Einstein model to the spectra of extended x-ray absorption fine structure (EXAFS) to study how pressure and temperature affect the cumulants and thermodynamic parameters of copper, silver, and their alloys. The parameters for the effective interatomic potential are derived by using the second-cumulant approximation, which includes contributions from all nearest neighbors of the absorbing and scattering atoms. The calculated thermodynamic parameters and effective anharmonic potential are consistent with those obtained experimentally and from other theories. The results prove that the anharmonicity of the thermal vibration of atoms is an essential contribution to the thermodynamic parameters and the EXAFS second cumulant at high temperature for ambient pressures up to 14 GPa. Increasing pressure reduces the EXAFS amplitude by reducing the atomic mean-square relative displacement (MSRD), which characterizes the EXAFS second cumulant (i.e., the Debye–Waller factor).

Keywords: anharmonic; CuAg72 alloy; pressure; second cumulant; thermodynamic parameters

I. Introduction

Extended x-ray absorption fine-structure spectroscopy has developed into a powerful probe of atomic structure and the high-temperature thermodynamics of substances due to anharmonicity.[1, 2] Numerous methods have been developed to investigate how temperature affects the EXAFS cumulants, such as path-integral effective-potential theory,[3] the statistical moment method,[4] the ratio method,[5] the Debye model,[6] the Einstein model,[7] and the anharmonic correlated Einstein model (ACEM).[8] Several groups have applied ACEM theory to EXAFS to study how the doping ratio affects the dependence of thermodynamic properties on temperature.[9–12] However, no reports yet exist that discuss how the thermodynamic parameters and the second cumulants depend on temperature and pressure for copper (Cu) doped with silver (Ag) for the ratio in the alloy CuAg72. The CuAg alloy contains elemental Cu and Ag, with the Ag atoms referred to as the substitution atoms and the Cu atoms referred to as the host atoms. The formula CuAg72 indicates a ratio of 72% Ag and 28% Cu (± 1%) atoms in the alloy and is also referred to as *CuSil* or *UNS P0772*. It is a eutectic alloy primarily used for vacuum brazing (note *CuSil*; not to be confused with *Cusil-ABA*, which has the composition 63.0% Ag, 35.25% Cu, 1.75% Ti).[9]

This study uses the effective anharmonic potential in ACEM theory applied to EXAFS[8] to investigate how the cumulants that contain the second cumulant [or Debye–Waller factor (DWF)] depend on temperature when subjected to high pressure. In addition, the study investigates the thermodynamic parameters, effective force constants, thermal expansion coefficient, correlated Einstein frequency, and correlated Einstein temperature, and how these parameters of the CuAg72 alloy depend on temperature under ambient pressure and high pressure. The numerical results are compared with experimental results and with the results of other studies.

II. Formalism

The EXAFS oscillation function is usually derived by using the cumulant-expansion approach, which contains the second cumulant σ^2 (or DWF) corresponding to the parallel

mean-square relative displacement (MSRD).[5] The second cumulant is an important factor in the analysis by EXAFS because the thermal lattice vibrations strongly influence the EXAFS amplitudes through the function $e^{-2\sigma^2 k^2}$.[1,13] One method to investigate how temperature affects the EXAFS cumulant is to combine ACEM with EXAFS,[8] which gives results that are consistent with experiments. The ACEM uses the effective interaction potential

$$V_E(x) \approx \frac{1}{2} k_{eff} x^2 + k_{3eff} x^3 + \ldots, \tag{1}$$

where k_{eff} is effective spring force constant, k_{3eff} is the effective cubic parameter that produces the anharmonicity that leads to asymmetry in the pair-distribution function, $x = r - r_0$ is the net departure of the instantaneous bond length between intermediate atoms from the equilibrium length or from the location of the minimum interaction potential, *r* is the spontaneous bond length between absorbing and backscattering atoms, and r_0 is the equilibrium value of r. The ACEM is determined by the vibration of single pairs of atoms, with M_1 and M_2 being the mass of the absorber and backscattering atom, respectively. The oscillation of the absorber and backscattering atom depends on their neighbors, so the interaction potential in Eq. (1) is written in the form of an anharmonic effective interaction potential $V_E(x)$:

$$V_E(x) = V(x) + \sum_{i=0,1} \sum_{j \neq i} V\left(\frac{\mu}{M_i} x \hat{R}_{01} . \hat{R}_{ij} \right), \tag{2}$$

where V(x) describes the interaction potential between absorbing and backscattering atoms, the sum *i* is over absorber ($i = 1$) and backscattering ($i = 2$) atoms, the sum j is over all nearest neighbors whose contributions are described by the term V(x), excluding the absorber and backscattering atoms themselves, M_i is the atomic mass of atom *i*, μ is the reduced atomic mass, and $\hat{R}$ is the unit vector for the bond. Therefore, this effective pair potential describes not only the interaction between absorber and backscattering atoms but also how the nearest-neighbor atoms affect such interactions, which is the difference between the effective potential used herein and the single-pair potential[14] and single-bond potential,[7] which only consider each pair of immediate-neighboring atoms [i.e., only V(x)] without considering the remaining terms on the right-hand side of Eq. (2). The atomic vibration is calculated by using a quantum statistical approach with an approximate quasi-harmonic

vibration in which the system Hamiltonian includes a harmonic term H_0 with respect to the equilibrium at a given temperature plus an anharmonic perturbation:

$$H = H_0 + V_E(a) + \delta V_E(a). \tag{3}$$

Here, the interaction potential $V_E(a)$ and anharmonic perturbation $\delta V_E(a)$ are

$$V_E(a) = k_{eff}a^2/2 + k_{3eff}a^3, \quad \delta V_E(a) = (k_{eff} + 3k_{3eff}a^2)y + k_{3eff}y^2,$$

where *a* is the thermal expansion coefficient with $a = \langle x \rangle, y = x - a, \langle y \rangle = 0$. Equation (3) leads to the ACEM interactive potential

$$V_E(x) = V_E(a) + k_{eff}y^2 + \delta V_E(y). \tag{4}$$

The ACEM interactive potential is the anharmonic potential of Morse pairs, which is appropriate for approximating the structure of cubic crystals. The Morse anharmonic potential is

$$V(r) = D\left(e^{-2\alpha(r-r_0)} - 2e^{-\alpha(r-r_0)}\right) = D\left(e^{-2\alpha x} - 2e^{-\alpha x}\right), \tag{5}$$

where $D(eV) = -V(r_0)$ is the dissociation energy and α_{12} ($Å^{-1}$) is the width of the potential. We expand Eq. (5) in *x* to obtain the third-order term that describes approximately the cubic structure of doped crystals. At the same time assume, when only considering crystals with orderly doping, the lattice is not corrupted, and we designate Cu as the host atom with indicator 1 and Ag as the substituted atom with indicator 2. The ACEM uses the Morse anharmonic pair potential to describe the pair interaction between atoms:

$$V_E(x) = D_{12}(e^{-2\alpha_{12}x} - 2e^{-\alpha_{12}x}) \approx D_{12}\left(-1 + \alpha_{12}^2x^2 - \alpha_{12}^3x^3 + ...\right). \tag{6}$$

For simplicity, we approximate the parameters of the Morse potential in Eq. (6) at a given temperature by $D_{12} = c_1D_1 + c_2D_2$, $\alpha_{12} = \sqrt{(D_1\alpha_1^2 + D_2\alpha_2^2)/(D_1 + D_2)}$, where c_1, c_2 are the doping ratios (%) of the alloy. We calculate the sums in the second term of Eq. (2) and compare the results with the terms of Eqs. (1) and (6) to obtain the effective force constant $k_{eff} = 5D_{12}\alpha_{12}^2$ of the effective anharmonic potential. At ambient pressure, the effective force constant is $k_{eff}^0 = 23D_{12}\alpha_{12}^2/4$.

To derive analytical expressions for the cumulants containing the second cumulant, we use perturbation theory.[13] Atomic vibrations are quantized as phonons, and the phonon-phonon

interaction leads to anharmonicity, with the phonon vibration frequency (i.e., the dispersion relation) taking the form

$$\omega(\mathrm{q}) = 2\sqrt{\mathrm{k}_{\mathrm{eff}}^{0} / \mu_{12}}\left|\sin\left(\mathrm{qa}_{0} / 2\right)\right|, \quad \left|\mathrm{q} \le \pi / \mathrm{a}_{0}\right|, \tag{7}$$

where a_0 is the lattice constant at temperature T, and q is the phonon wave number. The correlated Einstein frequency and correlated Einstein temperature at ambient pressure are respectively

$$\omega_{\mathrm{E}}^{0} = 2\sqrt{\mathrm{k}_{\mathrm{eff}}^{0} / \mu_{12}}\,, \qquad \theta_{\mathrm{E}}^{0} = \hbar\omega_{\mathrm{E}}^{0} / \mathrm{k}_{\mathrm{B}}\,. \tag{8}$$

By using these results in first-order thermodynamic perturbation theory,[12] we obtain the following cumulants under ambient-pressure conditions:

- The first cumulant or net thermal expansion is

$$\sigma^{(1)} = \frac{3\hbar\omega_{\mathrm{E}}^{0}}{40\,\mathrm{D}_{12}\alpha_{12}}\frac{\left(1+\mathrm{z}\right)}{\left(1-\mathrm{z}\right)}. \tag{9}$$

- The second cumulant (DWF) or MSRD is

$$\sigma^{(2)} = \frac{\hbar\omega_{\mathrm{E}}^{0}}{10\mathrm{D}_{12}\alpha_{12}^{2}}\frac{\left(1+\mathrm{z}\right)}{\left(1-\mathrm{z}\right)}. \tag{10}$$

- The third cumulant is

$$\sigma^{(3)} = \frac{3\hbar^{2}\left(\omega_{\mathrm{E}}^{0}\right)^{2}}{200\mathrm{D}_{12}^{2}\alpha_{12}^{3}}\frac{\left(1+10\mathrm{z}+\mathrm{z}^{2}\right)}{\left(1-\mathrm{z}\right)^{2}}. \tag{11}$$

- The thermal-expansion coefficient of the doped metal is

$$\alpha_{\mathrm{T}} = \frac{3\mathrm{k}_{\mathrm{B}}}{20\,\mathrm{D}_{12}\alpha_{12}\,\mathrm{r}}\frac{\mathrm{z}\ln\mathrm{z}^{2}}{\left(1-\mathrm{z}\right)^{2}}, \tag{12}$$

- The anharmonic factor at ambient-pressure is

$$\beta = \frac{9\eta\mathrm{k}_{\mathrm{B}}\mathrm{T}}{16\,\mathrm{D}_{12}}\left[1+\frac{3\mathrm{k}_{\mathrm{B}}\mathrm{T}}{8\mathrm{D}_{12}\mathrm{R}\alpha_{12}}\left(1+\frac{3\mathrm{k}_{\mathrm{B}}\mathrm{T}}{8\mathrm{D}_{12}\mathrm{R}\alpha_{12}}\right)\right], \qquad \eta = \frac{2\mathrm{z}}{1+\mathrm{z}}. \tag{13}$$

The second cumulant σ^2 contribution to the MSRD determining the anharmonic contribution to the EXAFS amplitude, $\sigma^{(1)}$, $\sigma^{(3)}$ contribution to the phase shift of the EXAFS due to anharmonicity. Note that $\sigma^{(1)}$, $\sigma^{(3)}$, and α_{T} contain the anharmonicity parameter $\mathrm{k}_{3\mathrm{eff}}$ and

only exist when this parameter is included, which is why $\sigma^{(1)}$, $\sigma^{(3)}$, and α_T must be considered when calculating the anharmonic effects in EXAFS. Under ambient-pressure conditions, the factor β is proportional to the temperature and inversely proportional to the shell radius, which is consistent with the anharmonicity obtained in experimental research into catalysis[15] if R is considered as the particle radius. In Eqs. (9)–(13), $z = \exp\left(-\theta_E^0 / T\right)$ is the heat function, which describes how the cumulants, the thermal expansion coefficient, and the anharmonic factor depend on the absolute temperature T and pressure applied to the doped metals.

III. Results and discussion

For Cu-Cu and Ag-Ag pure metals and the alloy CuAg72, Table I gives the calculated and experimental[16] parameters of the Morse potential, D_{12} and α_{12}, respectively.

TABLE I. Parameter of Morse potential for pure metals and their crystalline alloy.

Crystal	D_{12}(eV)	$D_{12}^{expt.}$(eV)	α_{12}(Å^{-1})	$\alpha_{12}^{Exp.}$(Å^{-1})
Cu-Cu	0.3429	0.3528	1.3588	1.4072
Ag-Ag	0.3323	0.3253	1.3690	1.3535
CuAg72	0.3381		1.3634	

Substituting the parameters D_{12} and α_{12} from Table I into Eq. (8), with the Boltzmann constant $k_B = 8.617 \times 10^{-5}$ eVÅ^{-1} and Planck's constant $\hbar = 6.5822 \times 10^{-16}$ eV.s, we calculate the values of the local force constant, Einstein frequency, and Einstein temperature at ambient pressures up to 14 GPa for Cu-Cu, Ag-Ag, and CuAg72 crystals. Table II lists the results, where $k_{eff}^{expt.}$ is the local force constant deduced from results of Okube *et al.*[17,18]

TABLE II. Effective parameters describing anharmonicity.

Crystal	k_{eff}(eVA^2)	$k_{eff}^{Expt.}$(eVA^2)	k_{eff}^0(eVA^2)	ω_E(10^{13}Hz)	ω_E^0(10^{13}Hz)	θ_E(K)	θ_E^0(K)
Cu-Cu	3.1655	3.4931	3.6403	3.0889	4.7710	236	364
Ag-Ag	3.1139	2.9797	3.5810	3.3933	3.6585	176	279

CuAg72	3.1423	3.6138	2.6874	4.3623	207	333

Inserting the thermodynamic parameters from Tables I and II into Eqs. (1) and (9)–(13) gives the effective anharmonic potential $V_E(x)$ as a function of the departure x from equilibrium bond length (see Fig. 1). The cumulants $\sigma^{(n)}(n)$, including the second cumulant or DWF, depends on the absolute temperature T and are influenced by pressure up to 14 GPa (see Figs. 2–5). Figure 6 shows the thermal expansion coefficient $\alpha(T,p)$ as a function of absolute temperature T and for various ambient pressures. Finally, Fig. 7 shows the anharmonic factor $\beta(T,p)$.

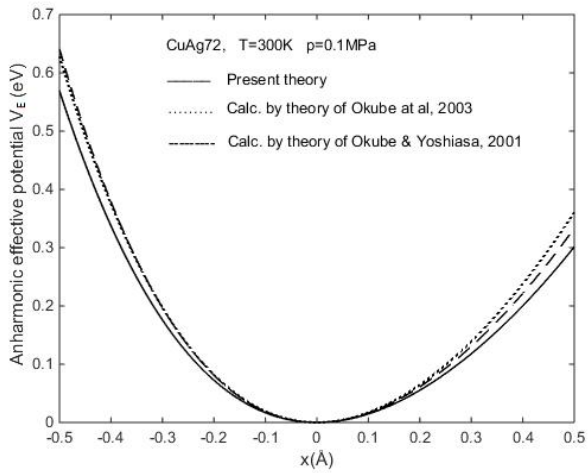

FIG. 1. Anharmonic effective potential $V_E(x)$ of CuAg72 as a function of departure x from equilibrium bond length. The result of the present theory is compared with results from other theories.

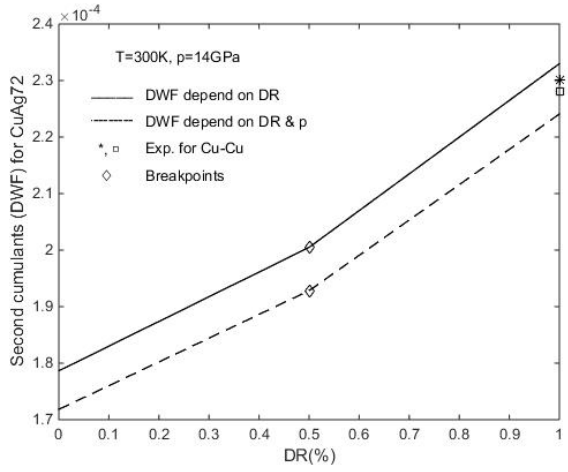

FIG. 2. Second cumulant σ^2 (DWF) for CuAg72 as a function of doping ratio DR.

Figure 1 compares the calculated anharmonic effective Morse potential $V_E(x)$ for the CuAg72 alloy at 300 K, 0.1 MPa (solid lines) with results from the theories of Okube *et al.*[18] (dotted curve) and Okube and Yoshiasa[17] (dashed curve) at the same temperature and pressure. The curves calculated for the Morse potential align closely with those obtained from the theories of Refs. [17,18], indicating that the coefficients k_{eff}, k_{3eff}, and k_{eff}^0 calculated by using the ACEM (given in Table II) are in reasonable agreement with measurements and the calculations of Okube *et al.* for CuAg72 alloy.

Figure 2 shows our calculation of the second cumulant or DWF as a function of doping ratio (DR) at 300 K and an ambient pressure of 14 GPa for the crystalline alloy CuAg72. These results illustrate that, for DRs of 0% to 50% and from 50% to 100%, the DWF values are

linear in DR (with different slopes in each range). For DR = 100% (i.e., where the Ag content is 0% and the Cu content is 100%) the calculated values are in good agreement with experimental values determined at 300 K (see symbols *, □).[19–21] However, there are breakpoints in the lines at 50% DR, which means that we do not have ordered atoms at DR = 50%. Thus, the Cu-Ag alloy does not form an ordered phase at the molar composition of 1:1 (i.e., the alloy CuAg50 does not exist).

This result is consistent with the findings of Kraut and Stern.[10] As the ambient pressure increases up to 14 GPa, the DWF decreases. For 0% Ag, 100% Cu, and 101 Kpa - normal atmospheric pressure (14 GPa) ambient pressure, DWF = 0.2330 Å^2 (0.2241 Å^2). With 100% Ag, 0% Cu, and 101 Kpa (14 GPa) ambient pressure, DWF = 0.1796 Å^2 (0.1718 Å^2). At the breakpoints, DWF = 0.2005 Å^2 and 0.1928 Å^2 at 101 Kpa and 14 GPa ambient pressure, respectively. Thus, increasing the ambient pressure decreases the EXAFS amplitude by reducing the atomic mean-square relative displacement that characterizes the EXAFS second cumulant (or DWF).

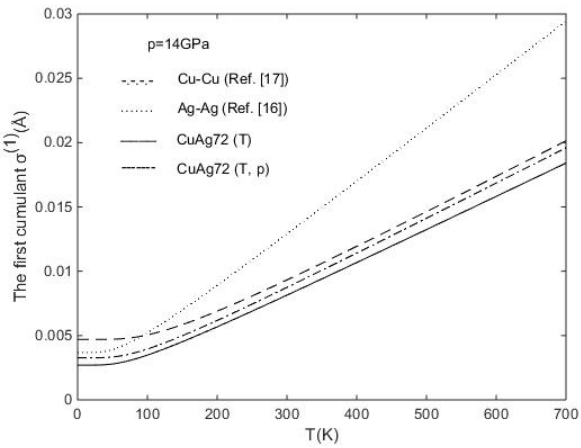

FIG. 3. First cumulant as a function of temperature for Cu, Ag, and CuAg72 at normal pressure and at 14 GPa ambient pressure.

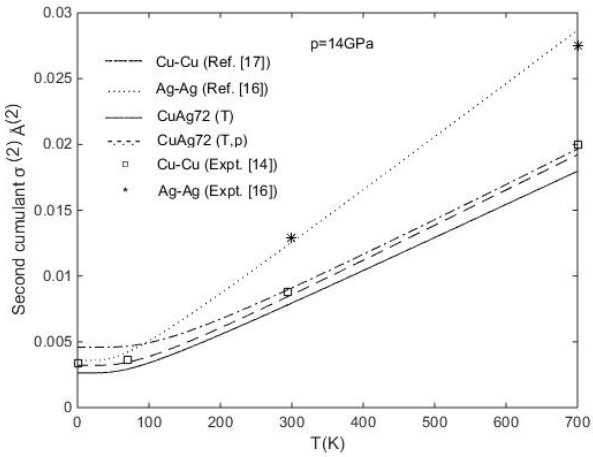

FIG. 4. Second cumulant (DWF) as a function of absolute temperature for Cu, Ag, and CuAg72 at 14 GPa ambient pressure.

Figure 3 shows the calculated first cumulant or net thermal expansion coefficient $\sigma^{(1)}$ as a function of temperature for Cu, Ag, and CuAg72 at normal pressure and at ambient pressures up to 14 GPa. At approximately the zero point with 101 Kpa normal atmospheric pressure and 14 GPa ambient pressure, $\sigma^{(1)} = 0.0027$ and $\sigma^{(1)} = 0.0047$ Å, respectively. At 700 K, $\sigma^{(1)} = 0.0184$ Å and $\sigma^{(1)} = 0.0201$ Å, respectively. Thus, as the pressure increases, the net thermal expansion coefficient also increases, but at low temperature the net thermal

expansion coefficient deviates more, meaning that the pressure causing the net thermal expansion is more pronounced at low temperatures.

Figure 4 shows the calculated second cumulant $\sigma^{(2)}$ or DWF as a function of absolute temperature for Cu-Cu, Ag-Ag, and CuAg72 and compares these results with experimental results[19,20] obtained at ambient pressure. The calculated values for the first cumulant (Fig. 3) and the DWF (Fig. 4) for different DRs and for an ambient pressure up to 14 GPa are proportional to temperature above about 100 K.

Consider the change in the second cumulant (DWF) for different temperatures: At approximately 0 K, the DWF increases from $\sigma^{(2)}$ = 0.0026 Å^2 to $\sigma^{(2)}$ = 0.0046 Å^2 as the pressure increases from normal atmospheric pressure up to 14 GPa. At 700 K, the DWF increases from $\sigma^{(2)}$ = 0.018 Å^2 to $\sigma^{(2)}$ = 0.0197 Å^2 as the pressure increases from normal atmospheric pressure up to 14 GPa. At low temperatures, the DWF changes more than at high temperatures because the change in ambient pressure from 101 Kpa to 14 GPa causes a greater relative mean-square displacement of atoms (MSRD or second cumulant $\sigma^{(2)}$) at low temperature than at high temperature. Furthermore, Fig. 4 shows that, from room temperature upward, the DWF remains almost constant as the ambient pressure increases, so the ambient pressure has a stronger effect at low temperatures. At low temperatures, $\sigma^{(2)}$ is very small and contains zero-point contributions that result from an asymmetry of the atomic interaction potential of these crystals due to anharmonicity.

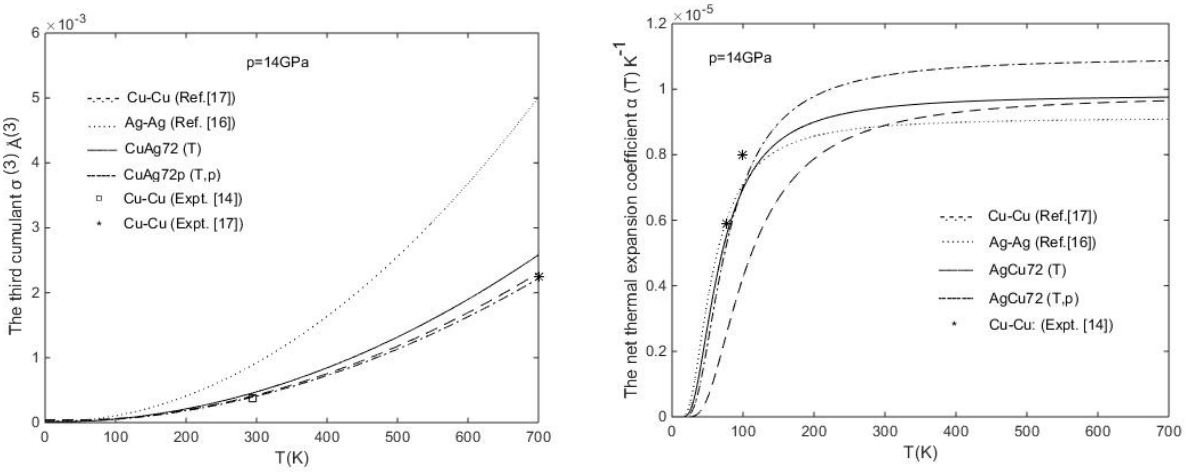

FIG. 6. Net thermal expansion coefficient for Cu, Ag, and CuAg72 as a function of absolute temperature and for various ambient pressures.

Figure 5 shows the calculated third cumulant $\sigma^{(3)}$ for Cu-Cu, Ag-Ag, and CuAg72 alloy as a function of absolute

temperature and at normal atmospheric pressure of 101 KPa and at an ambient pressure of 14 GPa. The calculated results for Cu-Cu and Ag-Ag are consistent with experimental results[19–21] at normal atmospheric pressure. At 0 K, for both 101 Kpa and 14 GPa ambient pressure, the third cumulant $\sigma^{(3)} \approx 0$ but, as the temperature increases, $\sigma^{(3)}$ for CuAg72 have value decrease when pressure increase: at 700 K, $\sigma^{(3)} = 0.0026$ Å^3 at 101 Kpa and 0.0023Å^3 at 14 GPa. Thus, high ambient pressure reduces the asymmetry of the atomic interaction potential at higher temperatures.

The results shown in Figs. 3–5 for CuAg72 at all pressures are very similar to the results for Cu-Cu, demonstrating the consistency between theoretical and experimental results. The calculated first three cumulants contain zero-point contributions at low temperatures, even if the results at high pressure are consistent with established theories.[1,7,8,13]

Figure 6 shows our calculated thermal expansion coefficient α_T for Cu-Cu, Ag-Ag, and CuAg72 as a function of absolute temperature with effects of ambient pressures. The calculated results for Cu-Cu are consistent with experimental results[19] at normal atmospheric pressure; however, the result for CuAg72 is deflected from 70 to 400 K when the ambient pressure is 14 GPa, which shows that, due to effect at high pressure, the thermal expansion coefficient α_T for CuAg72 is significantly reduced in the room-temperature range. However, the thermal expansion coefficient for CuAg72(T) and CuAg72 (T,p) changes very little at high pressure when the temperature exceeds 700 K.

The graph of α_T has the form of the specific heat C_V even at ambient pressure, thus reflecting the fundamental principle of solid-state theory, which states that thermal expansion results from anharmonic effects and is proportional to the specific heat C_V.[13] Our calculated values of α_T approach the constant value α_T^0 at high temperatures and vanish exponentially with θ_E / T at low temperatures, which is consistent with the results of previous research.[20,21]

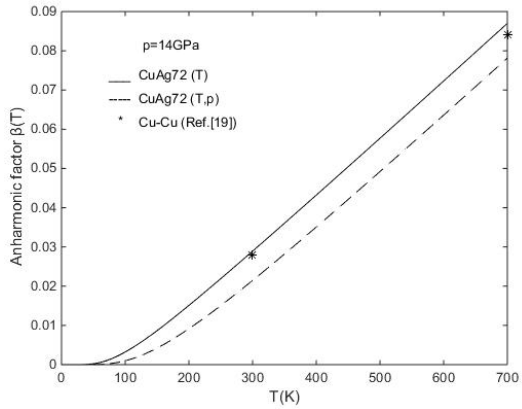

FIG. 7. Anharmonic factor for CuAg72 as a function of absolute temperature and for different ambient pressures.

Figure 7 shows the anharmonic factor $\beta(\mathrm{T})$ as a function of absolute temperature and for different ambient pressures for CuAg72. For both normal and high pressure (14 GPa), $\beta(\mathrm{T})$ is negligibly small at low temperature and increases strongly when the temperature exceeds the Einstein temperature. At normal atmospheric pressure, θ_{E} = 176 K for Ag, θ_{E} = 236 K for Cu, and θ_{E} = 207 K for CuAg72. At high pressure θ_{E}^{0} = 279 K for Ag, θ_{E}^{0} = 364 K for Cu and θ_{E}^{0} = 333 K for CuAg72. The results shown in Fig. 7 are consistent with experimental results,[19] which demonstrates that our calculations for CuAg72 are appropriate for normal atmospheric pressure. At temperatures above the Einstein temperature and for increasing ambient pressure, the anharmonic factor $\beta^{0}(\mathrm{T})$ is less than at normal pressure [$\beta(\mathrm{T})$], in other words, $\beta^{0}(\mathrm{T}) = 0.3125\,\beta(\mathrm{T})$ at 100 K, $\beta^{0}(\mathrm{T}) = 0.7439\,\beta(\mathrm{T})$ at 300 K, and $\beta^{0}(\mathrm{T}) = 0.898\,\beta(\mathrm{T})$ at 700 K. Thus, the anharmonic factor describes the temperature dependence of the anharmonic effects in EXAFS theory under influence of high ambient pressure.

IV. Conclusions

In this work, based on quantum statistical theory and by applying the effective anharmonic correlated Einstein model to extended x-ray absorption fine structure spectra, we derive analytical expressions for the temperature dependence of the cumulants and thermodynamic parameters of crystalline Cu, Ag, and their alloy CuAg72 at ambient pressures up to 14 GPa. The expressions for the second cumulant, the thermodynamic parameters, the effective force constant, the correlated Einstein frequency, and the correlated Einstein temperature for Cu,

Ag, and CuAg72 all agree with the known properties for these quantities. The expressions for calculations involving orderly doped crystals have forms similar to those for pure crystals.

Figures 1–7 show the cumulants and thermodynamic parameters for doped crystals as functions of absolute temperature and for ambient pressure. The results reflect the effect of anharmonicity in EXAFS and are consistent with results obtained in previous studies. The calculated results are also consistent with experimental results of other studies of Cu and Ag, and the results for the CuAg72 alloy are coherent. Thus, the method developed herein, which is based on applying the ACEM to EXAFS, is appropriate for calculating and analyzing the cumulant and thermodynamic properties of doped crystals.

References

[1] J. J. Rehr, Rev. Mod. Phys., 72, 621 (2000).

[2] Y. Iwasawa, K. Asakura, and M. Tada (Springer International Publishing, Cham., 2017).

[3] T. Yokoyama, J. Synchrotron Radiat. 6, 323 (1999).

[4] V. V. Hung, H. K. Hieu, and K. Masuda-Jindo, Comput. Mater.Sci., 49, 5214 (2010).

[5] G. Bunker, Nucl. Instrum. Methods Phys. Res. 207, 437 (1983).

[6] G. Beni and P. M. Platzman, Phys. Rev. B, 14, 1514 (1976).

[7] A. I. Frenkel and J. J. Rehr, Phys. Rev. B 48, 585 (1993).

[8] N. V. Hung and J. J. Rehr, Phys. Rev. B 56, 43 (1997).

[9] A. Nafi, M. Cheikh, and O. Mercier, J. Adhes. Sci. Technol. 27, 2705 (2013).

[10] J. C. Kraut and W. B. Stern, J. Gold Bulletin 33, 52 (2000).

[11] N. B. Duc, V. Q. Tho, N. V. Hung, D. Q. Khoa, and H. K. Hieu, Vacuum 145, 272 (2017).

[12] N. V. Hung, N. B. Trung, and N. B. Duc, J. Materials Sci. and Appl. 1, 91 (2015).

[13] N. B. Duc, H. K. Hieu, N. T. Binh, and K. C. Nguyen, X-Ray Absorption Fine Structure: Basic and Applications (Sciences and Technics Publishing House, Hanoi, 2018).

[14] J. M. Tranquada and R. Ingalls, Phys. Rev. B 28, 3520 (1997).

[15] B. S. Clausen, L. Grabæk, H. Topsoe, L. B. Hansen, P. Stoltze, J. K. Norskóv, and O. H. Nielsen, J. Catal. 141, 368 (1993).

[16] E. Benassi, Chem. Phys. 515, 323 (2018).

[17] M. Okube and A. Yoshiasa, J. Synchrotron Radiat. 8, 937 (2001).

[18] M. Okube, A. Yoshiasa, O. Ohtaka, and Y. Katayama, High. Press. Res. 23, 247 (2003).

[19] N. V. Hung, N. B. Duc, and R. R. Frahm, J. Phys. Soc. Jpn. 72, 1254 (2002).

[20] N. V. Hung and N. B. Duc, Proceedings of the Third International Workshop on Material Science (IWOM'S99, 1999).

[21] N. V. Hung and N. B. Duc, Commun. Phys., 10, 15 (2000).

[22] H.Ö. Pamuk and T. Halicioğlu, Phys. Stat. Sol. A 37, 695 (1976).